

# **Preventing Stress Corrosion Cracking and Enhancing Corrosion-Fatigue Performance of Steel and Aluminum by Laser Peening; deployment on nuclear spent fuel canisters.**

A Lloyd Hackel<sup>1</sup>, B. Jon Rankin<sup>1</sup>, C Matt Walter<sup>1</sup>, D Brent Dane<sup>1</sup>

<sup>1</sup> Curtiss-Wright Surface Technologies, 222 Mountain Vista Parkway, Livermore, California, 94551, USA

## **Abstract**

We report test results showing that laser peening prevents chlorine induced stress corrosion cracking (CISCC) of welded 316L stainless steel and 5000 series aluminums. Our previous work shows similar success preventing cracking in Hastelloy 22, Inconel 600 and Inconel 690. Based on published work identifying the importance of deep (>1 mm) compressive stress to prevent pitting from transitioning into cracking, we provide measurements of the multi-mm depth of compressive stress generated by laser peening in these steel and aluminum materials. The stainless steels tests are important for multi-purpose canisters (MPCs) used for spent nuclear fuel storage and the aluminum panels have important applications in Navy ship and marine applications that have been plagued by sensitization cracking of 5000 series aluminums. Using ASTM G36 (2013) accelerated corrosive testing we decisively show that CISCC does not initiate in weld areas of 316L stainless steel that were laser peened. We further show that for 5083 and 5456 aluminums, laser peening inhibits sensitization and most importantly prevents crack initiation or growth in thermally exposed panels with treatment either before or after sensitization level exposures. The testing of both the stainless and aluminums clearly shows that cracking will initiate and grow in non-peened regions, will not initiate in laser peened areas and that all cracking arrests upon propagating from non-peened areas into laser peened areas. In our work, test panels were exposed to a solution of magnesium chloride at 155°C and rapidly showed extensive cracking in non-peened areas. Based on the results of this work, the laser peening technology was approved by the NRC and used to protect the spent nuclear fuel canisters for the San Onofre Nuclear Power Plant.

**Keywords** Laser peening, spent fuel storage, stress corrosion cracking, sensitized aluminum

## **Introduction**

Chloride induced stress corrosion cracking (CISCC) is a severe problem impacting many industries and applications including but certainly not limited to nuclear, oil and gas and maritime. For nuclear spent fuel storage, the Multi-Purpose Canister (MPC) design was conceptualized by the U.S. Department of Energy to be a single versatile package for the nuclear industry, equally suitable for on-site storage, transport, and permanent disposal in a future repository. These dry canisters are a temporary approach for storing high-level radioactive waste such as spent nuclear fuel that has been cooled for a required time in a liquid pool. The past and current industry design life of MPCs ranges between 60 and 80 years. The Nuclear Regulatory Commission (NRC) provided initial 20-year license for the facilities using qualified MPCs. Many facilities are applying for license extensions which range from 20 to 40 years.<sup>1,2</sup>

MPCs are typically made of S30400 (304) and 316L stainless steel: although resistant to corrosion, they are known to be susceptible to CISCC. They are roll-formed and welded to cylindrical shape and after loading with spent fuel, sealed with a welded lid. The cylinders are typically filled with an inert gas such as helium and are placed vertically or horizontally in concrete vaults to provide radiation shielding and air flow for passive cooling. The dry canister system is being used in over 20 countries.

CISCC is also of critical importance when evaluating metal alloy dependability. Aluminum derived alloys of 5000 series were introduced due to their high strength and corrosion resistance but have been found highly susceptible to thermally induced sensitization due to precipitation of  $\beta$  phase ( $Mg_2Al_3$ ) at grain boundaries.<sup>3</sup> Between 2001 and 2002, over 400 commercial marine vessels that were constructed from Al-5083 were found to have experienced severe pitting and stress corrosion cracking.<sup>4</sup> Corrosion cracking on Navy ships presents an enormous economic burden to repair or replace an entire subunit to improve reliability of the vessel.

### Chloride Induced Stress Corrosion Cracking

To occur this cracking is generally considered to require the presence of three concurrent factors: 1) material susceptible to CISCC, 2) a corrosive environment and 3) tensile stress above a threshold, for example, tensile stress developed in component welds. With respect to canister's environment, spent fuel storage is predominantly being done at reactor sites which are typically located near a body of water for reactor cooling. The CISCC develops and propagates perpendicular to the vector direction of tensile residual stress. Welding for example is a source of such tensile stress developing along the weld line direction as well as transverse to the weld seam. For welded canisters, the tensile stress developed during the weld cool-down exposes grain boundaries of the sensitive material to the corrosive environment. Parrot and Pits report that fracture mechanics tests have shown that CISCC propagation can begin at low stress intensities in the range of  $2 \text{ MPa}\sqrt{\text{m}}$  to  $10 \text{ MPa}\sqrt{\text{m}}$  and that crack propagation is strongly dependent on temperature but is relatively unaffected by stress intensity.<sup>5</sup> Chen and Kelly have developed predictions of the maximum size of a hemispherical pit in type 304 and 316 stainless steels after exposure to atmospheric conditions.<sup>6</sup> The results of the calculations agree well with several sets of data for near-seacoast exposures on three continents for exposure times out to 26 years. Further evaluations have placed maximum pit size at around 0.2 mm. For structures containing tensile residual stresses, the critical depth of localized corrosion to initiate would be in the range of  $<1\text{mm}$ .<sup>7</sup>

### Deep compressive stress key to prevent pitting and CISCC

It has been observed that a close relationship exists between pitting and stress corrosion cracking in steels.<sup>8</sup> The case for aluminum is the same. Pitting often initiates and advances beyond the surface of a component and then notoriously tends to trigger failures by fatigue or stress corrosion cracking. The electro-chemistry of reactions, such as chloride ions in austenitic stainless steels, drives the pitting corrosion.<sup>9,10</sup> The chlorine ion has been identified as a species which attacks or breaks down a protective film leading to localized dissolution. In both cases of peening as illustrated in Figure 1 the depth of compressive stress reaches the transition to tensile stress at about  $300 \mu\text{m}$  depth. This shallow depth is in the range for pits to grow, thus potentially making shallow peening more susceptible to IGSCC than actually no peening at all. A safety factor thereby dictates that the compressive stress layer extend several times deeper than the potential pit growth depth.

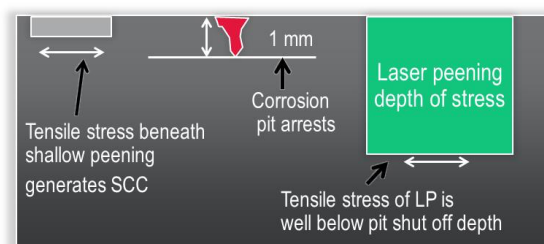


*Figure 1. Analyses and tests show corrosion pit depths will only penetrate to somewhat less than 1 mm before arresting. If the pitting penetrates beneath a shallow layer of peening and reaches tensile stress beneath, then cracking can initiate rapidly.*

### Dry canister test panel preparation, laser peening and residual stress measurement

Using the Holtec International preparation process of roll forming and welding, test panels of 316L stainless steel of 250 mm size by 16.5 mm thickness were fabricated. Figure 2 (5a) shows a plan view of a panel that was roll formed and welded per spent fuel canister fabrication procedures. The weld runs left to right. (5b) shows strongbacks that were lightly stitch-welded to the back of the plate to help provide similar constraints as found in the canisters, thus to hold the cylindrical shape from straining during the laser peening. Stitch welding was used to minimize stress generated during attachment of the stiffeners.



Figure 2. 5a. Canister test panel welded across width. 5b. Side-on view shows stiffening ribs used to help prevent straining as would be the case in the constraint of a canister

One panel was left in the as-welded condition and used for measurements of residual stress for the non-peened state. It was anticipated that the non-peened panel would have tensile stress in the welded area and this was confirmed by the measurement. A second panel was laser peened over the weld and heat affected zone (HAZ) area. Peening was done at 4 GW/cm<sup>2</sup> irradiance, 18 ns pulse duration and with 3 layers of coverage and use of aluminum tape ablative layer. Spot size of each laser pulse was 4.7 mm square (6.6 mm diagonal). Each layer of peening provides fully 100% coverage with the square laser spots robotically positioned within 0.1 mm precision of one next to another and using approximately 3% spot length overlaps. The peening area was 10 cm wide covering the weld and heat affected zones across the width of the panel. Residual stress measurements were performed across the full width of the panel by Hill Engineering using the two-dimensional Contour method<sup>11,12,13</sup> Guided by the FEA predictions, panels were laser peened with variations of process parameters and optimum process for canister peening was selected.

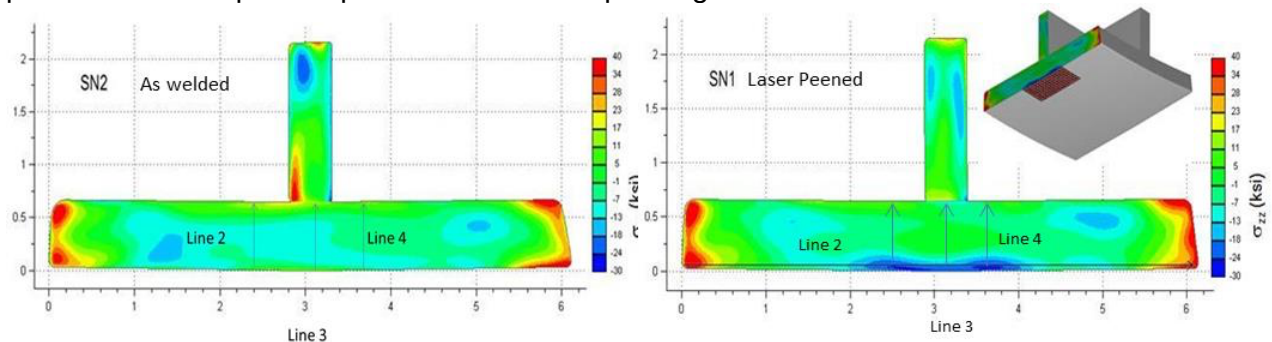


Figure 3. Contour measurement of residual stress in welded panels of 316L Stainless Steel. (SN1) was welded and then laser peened and (SN2) welded and left un-peened.

The left image of Figure 3 shows the stress profile in false-color for an as-welded non-peened panel. The depiction indicates tensile stresses in the 70 MPa (10 ksi) to 140 MPa (20 ksi) range as expected in the weld and heat affected zones. These would be of concern for stress corrosion cracking. In contrast, the right image shows measurement after laser peening of an identically welded panel. Three specific areas of importance are indicated with arrows where lineouts of the measured stress are graphically displayed in Figure 4.

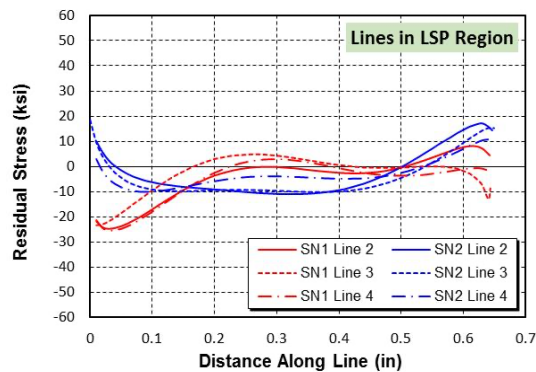


Figure 4. Lineouts of stress profiles of non-peened and laser peened panels measured by Contour. Laser peening converted tensile stress of up to 20 ksi (140 MPa) to 20 ksi (140 MPa) compressive and generated deep compression to 0.16 inch (4 mm) to .25 inch (6.2 mm) depth.

Comparing the lineouts it can be seen that the laser peening transformed these tensile areas to compressive (blue) residual stress in the weld area from approximately 175 MPa (25 ksi) tensile to 140 to 175 MPa (20 to 25 ksi) compressive. In the heat affected areas the transformation was from 140 MPa (20 ksi) tensile to 140 MPa to 175 MPa (20 to 25 ksi) compressive. Depth of compression in the weld zone extended to 4 mm (0.16 inches) to a deeper 5.6 mm (0.225 inches) in the heat affected zones.

But in measuring residual stress it is important to consider geometry. Peening of a constrained component will give more intense and deeper residual stress compared to identical peening of a sample with edges free to strain and thus relax some of the residual stress. Such is the case in measuring and relating the residual stress imparted by laser peening of a 316L unconstrained sample and that of the stress in a treated canister. Using our FE analysis we can calculate corrections. We relate measurements made in isolated panels to the actual stress computed by our FEA in the canister walls. In the methodology blocks 50 x 50 x 16 mm of 316L stainless steel, were fabricated and individually laser peened with 1, 2 or 3 layers of peening. Stress per layer of peening was then derived from slitting measurements. An FEA model of the canister was built and the laser peening results from the blocks applied in the model to specific canister areas. Stress in the canister and then stress in an unconstrained panel were calculated showing the increased stress retained in the canister. Figure 5 shows that the stress retained in the canister is approximately 2 mm deeper than that measured in the panel.

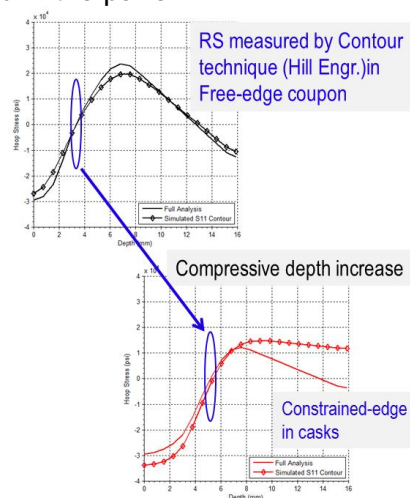


Figure 5. FEA analysis shows stress in a canister deeper than measured in free panel because the canister geometry constrains relaxation. In current case stress depth in a canister is 5.5 mm, that is 2 mm deeper than measured in a free panel.

### 5000 series aluminum test plates preparation

Aluminum 5083 and 5456 blocks of size 50 mm x 50 mm by 12 mm were fabricated for sensitization testing and 152 mm x 152 mm x 12 mm plates for SCC testing. For this application the peening was done with 4.7 mm square laser beam spots using 4 GW/cm<sup>2</sup> laser irradiance, with 18 nanosecond pulse duration and 2 layers of peening, calling this process 4-18-2 in our notation. Aluminum tape was used as the ablative layer. The sensitization test blocks were peened over all six surfaces for the G67 mass loss tests. The plates for SCC were peened on the top surface only and as in the previous tests, laser peening was performed on approximately one half of the plate exposure area leaving the other half non-peened. Because the plates did not contain welds for the SCC exposure, a tensile stress was applied by mechanically loading of individual plates. A steel rod was placed in between a reaction plate and the test plate and outboard bolts were used to load the surfaces to a stress of 80% of the Ultimate Tensile Strength (UTS) of the respective material. This resulted in pre-stressing the Al-5456 to 2597µε and the Al-5083 to 2200µε respectively.

### Stress Corrosion Cracking test setup

Tests were performed using a setup in the manner of ASTM G36-94<sup>14</sup> (Reapproved 2013). The corrosive exposure of the canisters in actual storage applications will be to their exterior surfaces as will sensitization exposure of 5000 series aluminum on Navy ships. For this reason an acceptably modified version of an ASTM G36 apparatus was used in which a glass cell with flanged open bottom was sealed with rubber o-rings and bolts to the “exterior” face of the test plate. Magnesium chloride crystals (MgCl<sub>2</sub>·6H<sub>2</sub>O) were inserted into the glass cell and heat applied to melt the crystals. To accelerate the corrosion exposure rate, a hot plate was placed underneath and heating coils were wrapped around the glass container to provide additional heating of the chloride liquid. A condenser cooled by separated flow from a chiller was inserted into the opening on top of the glass cell. A vapor trap containing a 25 weight percent solution of magnesium chloride was placed on top of the condenser to trap and reflux and thus minimize liquid loss. Power levels were adjusted on the hot plate and heating coils to melt the salt and bring the solution to a boil. The water-salt concentration was adjusted by adding water or allowing it to evaporate by temporarily removing the condenser until the boiling temperature reached a steady 155°C liquid level stabilized. Once the test apparatus was settled in, continuous operation at 155°C was straightforward to maintain and operate for long durations.

### Chloride Induces Stress Corrosion Cracking test of 316L

In the initial run, the cell was bolted to a section of plate that had a weld joint running across the diameter. The first test was of a non-peened area, run for 7 days and then cooled and the cell removed: extensive cracks were observed in the non-peened area. For the next test another welded panel was configured with one third of the exposure area partially laser peened and the remaining area left non-peened. This ensured that both peened and non-peened areas were identically exposed to the same conditions.

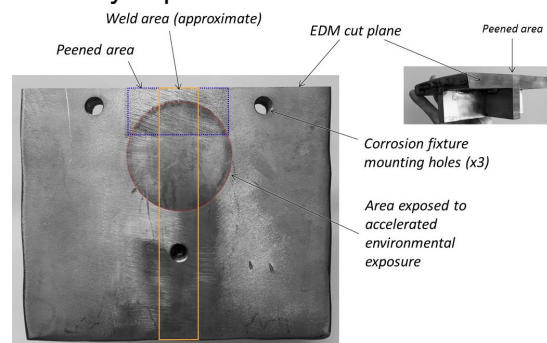
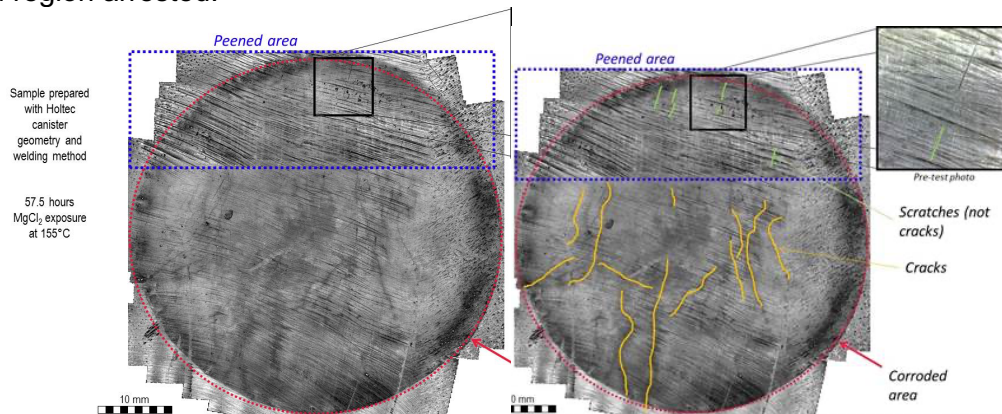


Figure 6. Welded test panel with laser peened and un-peened exposed areas



Figure 6 shows the test panel used. The weld and heat-affected zone ran vertically through the middle of the exposed area. After 57.5 hours exposure to the  $\text{MgCl}_2$  at  $155^\circ\text{C}$  heaters were turned off, the solution solidified and the cell removed allowing inspection of the panel. An array of photos was taken and stitched together with the resultant shown on the left side in Figure 7. The photo with the cracks highlighted is shown on the right. Cracks had extensively developed in the heat affected zone with some cracking in the weld area. No cracks developed in the laser peened region and cracks that propagated into the laser peened region arrested.



**Figure 7. Test plate of 316L stainless steel with and without highlighting of cracks.** Observation for cracking was made after 57.5 hours exposure to  $\text{MgCl}_2$  at  $155^\circ\text{C}$ . Cracks extensively developed in non-peened areas, did not develop in peened areas and arrested as they propagated from non-peened into peened areas. Pre-existing scratches in the peened region, identified by the green markings on the right, did not crack even though they would be considered prime candidates for initiation.

To quantify the potential of laser peening to prevent CISC over extended periods, a panel was laser peened over a 1/3 exposure area, leaving the remaining area non-peened and then similar testing was performed. After 18 hours exposure the panel was inspected to find that extensive panel cracking had already occurred. The apparatus then was reactivated and run to 342 hours total with no crack initiation or propagation into the laser peened area. The results indicate that even in extreme temperature and chlorine exposure, the laser peening will provide in excess of 19 times lifetime increase against CISC for the welds of 316L spent fuel canisters.

#### **ASTM G-67 sensitization test on 5000 series aluminum**

The criterion specified to determine the sensitization level of the aluminum is to expose a sample to an acid solution and measure the mass loss per unit area ( $\text{mg}/\text{cm}^2$ ) and compare it to the literature values for degree of sensitization; the greater the mass loss per unit area, the higher the degree of sensitization and the lower the weldability. Results indicate that the laser peened samples did not sensitize. Al-5083 sample that was laser peened on all six sides at 4-18-2 and then exposed for 14 days at  $100^\circ\text{C}$  had a mass loss of only  $11.61 \text{ mg}/\text{cm}^2$  compared to unpeened sample which lost  $47.51 \text{ mg}/\text{cm}^2$  after a shorter 8 day exposure. Another 5083 sample that was not laser peened but exposed for a total of 15 days lost  $21.55 \text{ mg}/\text{cm}^2$  whereas a second laser peened sample first exposed for 19 days and then an even longer 21 days lost respectively only  $12.39$  and  $20.82 \text{ mg}/\text{cm}^2$ .

#### **Stress Corrosion Cracking of sensitized 5000 series aluminum**

Using the G36 test apparatus exposures were made of both the Al 5456 and Al 5083, testing for cases of sensitized (exposed to sensitizing time and temperature). Samples were then laser peened and the complementary condition of laser peened first and then exposed to sensitizing time and temperature was evaluated. In this case of laser peening first, as for new ship construction, we do not here use the term sensitized because for the severe

exposures of our tests, the G67 data indicates the material did not sensitize after laser peening.

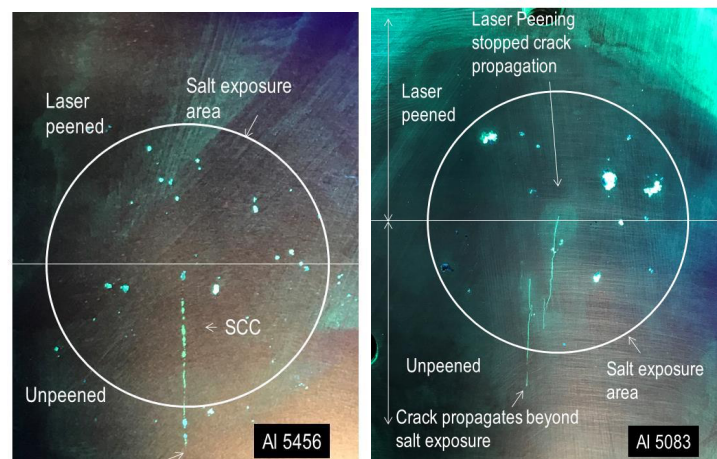


*Figure 8. Laser peening prevents CISCC cracking 5000 series Aluminums. Al5456 was sensitized and the laser peened. Al5083 was laser peened and then exposed to sensitization environment. Cracks developed and propagated in the non-peened region. No cracks developed in the laser peened region after 300 hours. Cracks in the peened region arrested as they encountered the compressive stress of the laser peened area.*

Sensitization cracking tests of Al-5456 were conclusive. Figure 8 left shows the Al 5456 test plate that was peened at 4-18-2 and was then sensitized it by thermal exposure at 100°C for 14 days. The plate was pre-stressed to 597 $\mu\epsilon$  and run in the G-36 test for 303 hours developing cracks in the non-peened region. Again cracking did not develop in the laser peened region and cracks from the non-peened region arrested as they propagated into the compressive stress of the peened area. A 152 x 152 mm plate of Al-5083 was first sensitized by exposing for 19 days at 100°C. Then approximately one half of its exposure area was laser peened at 4-18-2. Next the sample was loaded with strain gauge monitoring to a tensile strain of 2200 $\mu\epsilon$ . Considering Young's modulus of 70.3 GPa (10.2 Msi), a tensile loading stress of 155 MPa (22.4 ksi) was applied. Figure 14 right shows this panel cracked in the non-peened region after 96 hours of MgCl<sub>2</sub> exposure. Again cracks originating in the non-peened region arrested as the propagated into the laser peening.

### **Deployment of Laser Peening for nuclear spent fuel canisters**

Taking the technology beyond the qualifying laboratory tests and evaluations to field deployment was an important step for fully demonstrating the capability of the laser peening process to support nuclear applications. A highly automated laser and robotic system was configured to peen the welds of 75 MPCs for the San Onofre Nuclear Power Plant at the Holtec International canister fabrication facility. The right hand photo of Figure 9 shows the beam delivery hardware and robotics that precisely positioned the laser beam spots onto the canister. A rotation system rotated the canisters to peen the hoop welds and with rotation fixed, the delivery robot translated along a track for peening the longitudinal welds. Individual spots were placed on the canister with 0.1 mm precision and recordings made of laser energy and pulse duration for each shot. The canisters were peened with a 100 mm (4 inch) wide coverage at 4 GW/cm<sup>2</sup> irradiance, 18 ns pulse duration and 3 layers of coverage. The photo at right shows the laser peening system as deployed at the manufacturing facility. The UL qualified laser system is housed in a trailer and its output beam is propagated into a light safe tent and to the beam controller mounted on the delivery robot. The beam controller precisely conditions the spot and directs it on to the canister. The water delivery nozzle is attached to and move with the controller. Processing is controlled by operators at the external control station. Canisters were peened at the rate fabricated and the laser system returned to California home base when peening was completed.



*Figure 15. Laser peening system configured for treating welds of nuclear spent fuel canisters. At left beam director mounted on the robot (orange) for canister processing. At right system configured for field operation.*

## Conclusion

Our measurements and analysis for both the 316L and the 5000 series aluminums show that laser peening generates compressive stress to multi-mm depths, well beyond the self-terminating pit depth estimated at about 200  $\mu\text{m}$  due to cathodic current limits. Our accelerated ASTM G36 (2013) tests conducted at 155°C with  $\text{MgCl}_2$  clearly show that CISCC will not initiate in areas treated with high energy laser peening and that CISCC originating outside of a laser peened zone will arrest upon reaching the peened area. The current work includes stress intensity vs. depth generated from 2-dimensional residual stress measurements made by Hill Engineering using a Contour method. The high energy laser peening offers an excellent safety margin for structural integrity of spent fuel dry storage canisters and alleviates concerns related to cracking prior to moving canisters to a permanent repository facility. For marine applications laser peening alleviates CISCC of sensitized 5XXX aluminums and reopens using this higher strength aluminum for advanced systems.

## ACKNOWLEDGEMENT

Work on 5000 series aluminum supported in part by the Naval Shipbuilding Research Program

## References (

1. M.R. Wisenburg, "Use of multi-purpose casks for at-reactor spent fuel storage", Proceedings of the Institute of Nuclear Materials management (INMM) spent fuel seminar, p277, 13-15 January 1995, Washington DC.
2. B. Gutherman and D. LeDuc, "Summary of Design Criteria for Dry Cask Storage Systems for ISFSI storage of Shutdown Reactor Spent Nuclear Fuel," U.S. Department of Energy, Nuclear Fuels Storage and Transportation Planning Project, FDRC-NFST-2015-000538, Rev. 0, SRNL-TR-2015-00106.
3. E.H. Dix, Jr., W.A. Andersen, M.B. Shumaker, "Influence of Service Temperature on the Resistance of Wrought Aluminum-Magnesium Alloys to Corrosion", CORROSION, Vol. 15, No. 2, pp. 55t-62t, Feb. 1959.
4. H. Bushfield and M. Cruder, "Sensitized marine aluminum plate & ASTM standard specification B928-an update," in SNAME Section Meeting, 2006.
5. R. Parrott, R., and H. Pitts, H., "Chloride stress corrosion cracking in austenitic stainless steel", prepared for the Health and Safety Laboratory, Crown Publishing 2011. Copies can be found online at <http://www.hse.gov.uk/research/rrpdf/rr902.pdf>.
6. J.J. Truhan Jr., R.F. Hehenamm, "Surface Aspects of Pitting and SCC", NASA CR-135212, April 1977
7. M.T. Woldemedhim, M.E. Shedd, and R.G. Kelly., Evaluation of Maximum Pit Size Model on Stainless Steels under Thin film Electrolyte Conditions, J of the Electrochemical Society, 161(8), E3216-E3224, 2014.
8. J.J. Truhan Jr., R.F. Hehenamm, "Surface Aspects of Pitting and SCC", NASA CR-135212, April 1977



11. M.B. Prime, "Residual Stress Measurement by Successive Extension of a Slot: The Crack Compliance Method," *Applied Mechanics Reviews*, Vol 52, No. 2, pp. 75-96, 1999.
12. M. B. Prime, D. J. Hughes, P. J. Webster, "Weld Application of a New Method for Cross-Sectional Residual Stress Mapping", *Proc. 2001 SEM Annual Conference on Experimental and Applied Mechanics*, June 4-6, Portland, OR, pp. 608-611. (LA-UR-01-1244).
13. M.B. Prime, 2018, "[The Two-Way Relationship Between Residual Stress and Fatigue/Fracture](#)," *Fracture, Fatigue, Failure and Damage Evolution*, Volume 7: Proceedings of the 2017 Annual Conference on Experimental and Applied Mechanics, , pp. 19-23.35.
14. ASTM G36-94(2013), Evaluating Stress-Corrosion-Cracking Resistance of Metals and Alloys in a Boiling Magnesium Chloride Solution, ASTM International, West Conshohocken, PA, (2013), [www.astm.org](http://www.astm.org).